LRP 637/99 June 1999

Effect of $E \times B$ Flows on the Linear Stability of Ion Temperature Gradient Modes, Using a Global and Spectral Gyrokinetic Model

M. Maccio, J. Vaclavik

submitted for publication in

Physics of Plasmas

ISSN 0458-5895

Effect of $E \times B$ flows on the linear stability of ion temperature gradient modes, using a global and spectral gyrokinetic model.

M. Maccio*, J. Vaclavik

Centre de Recherches en Physique des Plasmas, Association Euratom - Confédération Suisse

Ecole Polytechnique Fédérale de Lausanne, PPB – CH-1015 Ecublens/Switzerland

(June 16, 1999)

Abstract

Strong electric fields generate an $E \times B$ rotation of the equilibrium plasma. Experiments have shown that this effect could lower the anomalous transport in tokamaks. The study of the effect of these flows on the linear stability of ion temperature gradient (ITG) modes has therefore been undertaken. The question is addressed solving the spectrum of the gyrokinetic equation in the full 2-dimensional poloidal plane. Results show a strong effect of $E \times B$ flows: they stabilize the ITG modes and reduce the extent of the convective cells. Study with respect to different profiles of the flow shows that the so-called curvature of flow (second derivative) has no effect, while the intensity of flow itself produces the strongest effect.

52.35.Kt, 52.25.Fi, 52.25.Dg, 52.35.-g

*E-mail: matteo.maccio@epfl.ch

I. INTRODUCTION

$E \times B$ sheared flows are widely held responsible for the creation of internal transport barriers in fusion devices. Thus, the anomalous transport should be reduced as a consequence of their presence [1]. On the other hand, micro-instabilities are a major candidate to explain the anomalous transport. It is therefore natural to study the effect of $E \times B$ sheared flows on micro-instabilities and particularly on the linear stability of ion temperature gradient (ITG) modes, in a toroidal geometry.

Previous work [2] on this question has shown that the ballooning transform is of no use for this. The simplest way to avoid this problem is to study the effect of these sheared flows in the full 2-dimensional poloidal plane. The first attempt to do so is a global and spectral fluid model [3] that addresses the question of the linear stability of ITG modes. This model has a important drawback: the lack of Landau damping, which allows plenty of slab-like ITG modes to exist even in the tokamak geometry. The slab-like modes being not strongly affected by the $E \times B$ flows, the results of the fluid model were rather disappointing, although a strong effect on the toroidal ITG modes could be seen, but not studied with much precision.

This motivated the present work, in which the same study is undertaken, but in the framework of the kinetic theory. We started from the gyrokinetic equation with strong electric fields that was obtained by Hahm [4] and solved it using the formalism developed by Brunner *et al.* [5]. This formalism solves the problem of linear stability of ITG modes in the full 2-dimensional poloidal plane. It includes the effects of finite Larmor radius (FLR) to all orders in a spectral approach.

The article is organized as follows: in Sec. II A we explain how to include $E \times B$ flows in the resolution of the gyrokinetic equation. Then, in Sec. II B we restrict ourselves to a large aspect ratio tokamak. Eventually, in Sec. III we present the results and discuss them.

II. GYROKINETIC MODEL

The plasma is modeled by gyrokinetic ions with full FLR effects and adiabatic electrons. We linearize the gyrokinetic equation for ions, including a strong equilibrium electric field. Then the quasi-neutrality approximation is used to couple the ions to the electrons, which are considered adiabatic. This results in an eigenvalue integral equation for the ITG modes with strong electric fields. The spectral problem is solved in the full 2-dimensional poloidal plane for a large aspect ratio tokamak.

A. General geometry

The first step is to include strong electric fields in the gyrokinetic formalism. This was done by Hahm [4] with the use of Hamiltonian mechanics in non-canonical variables and Lie transforms formalism. We solve this new gyrokinetic equation using a perturbation method, as we are interested in the linear stability problem.

In Ref.4, Hahm used the variables $\{\mathbf{R}, \alpha, \mu, v_{\|}, t\}$, being the guiding center position, the Larmor rotation angle, the magnetic moment, the parallel velocity and time respectively. But to simplify our linear calculations, we have decided to work with an "energy" variable ε instead of the parallel velocity $v_{\|}$, because, as we will see later, at the lowest order in perturbation, it is a constant. We define it as:

$$\varepsilon := e\phi_0 + m\mu B + \frac{m}{2}\left(v_{\|}^2 + \mathbf{u}^2\right) \tag{1}$$

where e and m are the ion charge and mass respectively, ϕ_0 is the potential for the strong electric field, B is the modulus of the magnetic field, $\mathbf{u}$ is the sheared $E \times B$ flow:

$$\mathbf{u} := \frac{1}{B^2}\mathbf{B} \times \nabla\phi_0 \tag{2}$$

The second step is to apply an electrostatic perturbation $< \delta\phi >$ to the equilibrium plasma; the notation $< \cdots >$ represents an averaging over α, which appears via the Lie transforms formalism. Given this, it is easily shown that:

$$\dot{\varepsilon} = -e\dot{\mathbf{R}} \cdot \nabla \left[< \delta\phi > (\mathbf{R}, \mu, t) \right] \tag{3}$$

where $\nabla = \partial_{\mathbf{R}}$ and we have [4]:

$$\dot{\mathbf{R}} = v_{||}\mathbf{e}_{||} + \mathbf{u} + \frac{1}{eB_{||}^{\star}} \left[m\mu\nabla B + m \left(v_{||}\mathbf{e}_{||} + \mathbf{u} \right) \nabla \left(v_{||}\mathbf{e}_{||} + \mathbf{u} \right) \right] \tag{4}$$

where $B_{||}^{\star} = B + (m/e)\mathbf{e}_{||} \cdot \mathrm{rot}(v_{||}\mathbf{e}_{||} + \mathbf{u})$ and $\mathbf{e}_{||} = \mathbf{B}/B$. It is possible to show, using the Lie transform formalism, that:

$$n_{ions}(\mathbf{x}, t) = \int B_{||}^{\star} \left[F + \frac{e}{mB} \delta\tilde{\phi} \partial_{\mu} F + f \right] \cdot \delta(\mathbf{R} + \rho_L - \mathbf{x}) d\mathbf{R} d\alpha d\mu dv_{||} \tag{5}$$

where $\mathbf{x}$ is the position of the particle and not the position of the guiding centers and with the following definitions: $\delta\tilde{\phi} = \delta\phi - < \delta\phi >$ and $\delta(\cdots)$ is the Dirac distribution.

With the $\{\mathbf{R}, \alpha, \mu, \varepsilon, t\}$ variables, the linearized gyrokinetic equation reads:

$$\partial_t f + \dot{\mathbf{R}} \cdot \nabla f = - \left[\frac{1}{B^2} \left(\mathbf{B} \times \nabla < \delta\phi > \right) \cdot \nabla F + \dot{\varepsilon} \partial_{\varepsilon} F \right] \tag{6}$$

where f is the first order perturbation part of the distribution function and F is the equilibrium part. We choose F to be a Maxwellian.

Eq.(6) can be formally solved by integrating over time along the equilibrium trajectories. To simplify the expressions, we first single out the adiabatic part of f, by defining the function g:

$$g := f + e < \delta\phi > \partial_{\varepsilon} F \tag{7}$$

which is the non-adiabatic part of the first order perturbation of the distribution function. We also use the fact that it is possible to write the electrostatic perturbation $< \delta\phi >$ as [5]:

$$< \delta\phi > (\mathbf{R}, \mu, t) = \exp(-i\omega t) \int_{\mathbb{R}^3} d\mathbf{k} \left[J_0(k_{\perp}\rho_L) \delta\hat{\phi}(\mathbf{k}) \exp(i\mathbf{k} \cdot \mathbf{R}) \right] \tag{8}$$

with $\omega \in \mathbb{C}$ representing the spectral approach and where $\delta\hat{\phi}(\mathbf{k})$ is the Fourier transform of the potential $\delta\phi(\mathbf{R}, \alpha, \mu)$, i.e. the electrostatic perturbation not averaged over α. The averaging over α is represented in the Bessel function.

Then the formal solution of Eq.(6) is:

$$g = -\frac{eF}{T_i}\int_{\mathbb{R}^3} d\mathbf{k}\left[J_0(k_\perp \rho_L)\exp\left(i\mathbf{k}\cdot\mathbf{R}(t) - i\omega t\right)(\omega - \omega^\star)\, i\mathcal{P}\cdot\delta\hat{\phi}(\mathbf{k})\right] \tag{9}$$

where T_i is the ion equilibrium temperature, J_0 is the Bessel function, $k_\perp$ the component of $\mathbf{k}$ which is perpendicular to the magnetic field, ρ_L is the ion Larmor radius and we have defined the following differential operator:

$$\omega^\star := -\frac{iT_i}{eB}\left[\mathbf{e}_n\cdot\nabla\left(\ln F\right)\right]\left[\mathbf{e}_b\cdot\nabla\right] \tag{10}$$

where $\mathbf{e}_n$ and $\mathbf{e}_b$ are the normal and binormal unit vectors respectively, defined with respect to the flux surfaces and the field lines of the magnetic field.

The propagator $\mathcal{P}$ is defined as [5]:

$$\begin{aligned}\mathcal{P}(\mathbf{R},\mathbf{k},\varepsilon,\omega) &:= \int_{-\infty}^{t} dt' \exp\left[i\mathbf{k}\cdot\left(\mathbf{R}(t') - \mathbf{R}(t)\right) - i\omega\left(t' - t\right)\right] \\ &= \int_{-\infty}^{t} dt' \exp\left[i\int_{t}^{t'}\left(\mathbf{k}\cdot\dot{\mathbf{R}}(t'') - \omega\right)dt''\right]\end{aligned} \tag{11}$$

At this point, we have a formal solution to perturbation calculation. It is worth noting that this formal solution is nowhere explicitly modified by the strong electric fields. In fact, this solution is exactly the same obtained by Brunner *et al.* in Ref.5. The only effect of the strong electric field is to modify the equations of motion of the guiding centers, thus modifying the trajectories, which explicitly appear in Eq.(11). Thus, all the details of the numerical resolution of the problem will be the same as in [5]. We only need to compute an explicit formula for the propagator with strong electric fields.

B. Large aspect ratio tokamak

We have restricted ourselves to the case of a large aspect ratio tokamak, with circular concentric flux surfaces. The magnetic field is taken as:

$$\mathbf{B}\left(\rho,\theta\right) = B_0\frac{R_0}{r(\rho)}\left(\mathbf{e}_\varphi + \frac{\rho}{R_0 q_s(\rho)}\mathbf{e}_\theta\right) \tag{12}$$

where R_0 is the major radius, $r(\rho) = R_0 + \rho\cos(\theta)$ is the cylindrical radius, B_0 is the magnetic field on the axis, $\mathbf{e}_\varphi$ is the unit vector along the toroidal angle, $\rho \in [0, a]$ is the minor radius,

θ is the geometric poloidal angle, $q_s(\rho)$ is the safety factor, which is chosen arbitrarily, and $\mathbf{e}_\theta$ is the unit vector along the poloidal angle. We assume that $a/R_0 \ll 1$.

The last step before the explicit computation of the propagator, is the determination of the equilibrium trajectories of the guiding centers, i.e. the computation of $\mathbf{R}(t')$. To solve the equations of motion, we use an iterative method, considering that the drifts are a correction to the unperturbed trajectories. In this geometry, the equilibrium equations of motion for the guiding centers read [Eqs.(4) and (12)]:

$$\begin{aligned}
\dot{\rho} &= -v_D \sin\theta + \frac{u^2(\rho)}{R_0\omega_{ci}} \sin\theta \\
\dot{\theta} &= \tilde{\omega}_t - \frac{v_D}{\rho}\cos\theta - \frac{u^2(\rho)}{\rho^2\omega_{ci}} \\
\dot{\varphi} &= \omega_t q_s(\rho)
\end{aligned} \tag{13}$$

where $\omega_t := v_\parallel / R_0 q_s(\rho)$ is the poloidal transit frequency and $\tilde{\omega}_t := \omega_t + u(\rho)/\rho$, ω_{ci} is the ion cyclotron frequency, $\{\rho, \theta, \varphi\}$ are the toroidal variables, and v_D is the magnetic drift:

$$v_D = \frac{1}{R_0\omega_{ci}} \left(B_0\mu + {v_\parallel}^2\right) \tag{14}$$

and $u(\rho)$ is obtained through (2) and (12):

$$\mathbf{u} = u(\rho)\left[1 + \frac{\rho}{R_0}\cos\theta\right]\mathbf{e}_\theta \tag{15}$$

From now on we will only consider highly passing ions and in order to solve the equations of motion, we will make the assumption that the parallel velocity is constant: $v_\parallel(t) = v_\parallel(t_0)\ \forall t$. Solving iteratively Eqs.(13) yields:

$$\begin{aligned}
\rho(t') - \rho(t) &= \frac{1}{\tilde{\omega}_t}\left(v_D - \frac{u^2}{R_0\omega_{ci}}\right)\left[\cos(\tilde{\omega}_t t') - \cos(\tilde{\omega}_t t)\right] \\
\theta(t') - \theta(t) &= \tilde{\omega}_t(t'-t) - \frac{u^2}{R_0\omega_{ci}}(t'-t) - \frac{v_D}{\rho\tilde{\omega}_t}\left[\sin(\tilde{\omega}_t t') - \sin(\tilde{\omega}_t t)\right] \\
\varphi(t') - \varphi(t) &= \omega_t q_s (t'-t)
\end{aligned} \tag{16}$$

These equations are what we were seeking: we can now safely proceed to the explicit computation of the propagator.

Before going further, we would like to point out that we have in fact used a toroidal wave decomposition, rather than the standard plane wave representation. Thus, Eq.(8) should read:

$$\int_{\mathbb{R}^3} d\mathbf{k} \left[\delta\hat{\phi}(\mathbf{k}) \exp(i\mathbf{k}\cdot\mathbf{R})\right] = \sum_{k,m\in\mathbb{Z}} \delta\hat{\phi}_{(k,m)} \exp\left[i\left(k\frac{2\pi}{\Delta\rho}\right)\rho + im\theta + in\varphi\right] \tag{17}$$

where $\Delta\rho = (\rho_{Max} - \rho_{min})$ and $[\rho_{min}, \rho_{Max}]$ are the boundary within which we solve the problem. m and n are the poloidal and toroidal wave numbers respectively and $n \in \mathbb{Z}$ is fixed because the problem is axisymmetric. This decomposition implies an approximation on the geometry, which implications are fully discussed in Ref.6.

Therefore, using Eq.(11), the iterative integration of the guiding centers trajectories and (17), it can be shown that the propagator becomes:

$$\mathcal{P}(\theta) = \sum_{p,p'\in\mathbb{Z}} J_p(x) J_{p'}(x) \frac{\exp\left[i(p-p')(\theta+\bar{\theta})\right]}{i\left(y - \omega + p\tilde{\omega}_t\right)} \tag{18}$$

where J_p are the Bessel functions and we have used the following definitions:

$$\begin{aligned} x &= \left[\left(k\frac{2\pi}{\Delta\rho}\right)^2 \frac{1}{\tilde{\omega}_t^2}\left(v_D - \frac{u^2}{R_0\omega_{ci}}\right)^2 + \left(\frac{mv_D}{\rho\tilde{\omega}_t}\right)^2\right]^{\frac{1}{2}} \\ y &= m\tilde{\omega}_t + nq_s\omega_t - m\frac{u^2}{\rho^2\omega_{ci}} = k_\parallel v_\parallel + m\frac{u}{\rho}\left(1 - \frac{u}{\rho\omega_{ci}}\right) \\ \cos\bar{\theta} &= \left(k\frac{2\pi}{\Delta\rho}\right)\frac{1}{\tilde{\omega}_t}\left(v_D - \frac{u^2}{R_0\omega_{ci}}\right)/x \\ \sin\bar{\theta} &= \left(\frac{mv_D}{\rho\tilde{\omega}_t}\right)/x \end{aligned} \tag{19}$$

where $k_\parallel := (m+nq_s)/(R_0 qs)$. Eq.(18) is all we needed: it is the expression of the propagator in presence of a strong electric field. The set of equation is now complete: using (5), (7), (9), (18), the quasi-neutrality approximation and the adiabatic electrons, we can produce an eigenvalue integral equation which considers the full 2-dimensional poloidal plane. It can be solved to determine the spectrum of the ITG modes in the framework of gyrokinetic theory. The details are to be found in Ref.5.

C. Numerical Implementation

To give a resume, we have solved the linearized gyrokinetic equation for ions, in a spectral approach. This solution coupled with the adiabatic electrons gives rise to an integral equation for the eigenmodes of the electrostatic potential. The free input data parameters for our problem are: the profiles of equilibrium quantities, the parameters of the equilibrium geometry, the toroidal wave number n, and the profile of the $E \times B$ sheared poloidal flow u.

Given these, the task is to find the eigenmodes of the plasma, i.e. find the values of ω for which there is a non-trivial solution $\delta\hat{\phi}$ to the integral equation. To find the eigenfrequencies in the complex plane we use an algorithm based on the Nyquist theorem.

Details on the numerical implementation can be found in Ref.5.

III. RESULTS

With our global and spectral formulation we can answer several questions about the effect of $E \times B$ sheared poloidal flows on the linear stability of ITG modes. In this article, we will study the effect of different shapes of the flow.

Let us first describe a typical study case; we chose the following parameters: $a = 0.21$[m], $R_0 = 1.19$[m], $B_0 = 1$[Tesla], $T_e = T_i = 1$[keV], the ions were hydrogen, $n = 7$, $q_s \in [1, 5]$ and $q_s \approx 2$ where the mode amplitude is maximum. The parameters are set so that the ITG toroidal modes are much more unstable than the ITG slab-like modes that exist even in toroidal geometry. In this study we are only interested in ITG toroidal modes.

Then, here is how we chose the profile of $E \times B$ poloidal flow:

$$u(s) = \text{Mach} \cdot v_{thi} \left[u_0 + u_1 s + u_2 s^2\right] \tag{20}$$

where v_{thi} is the ion thermal velocity and $s = \rho/a$ is the normalized radial variable. This allows to study separately the effect of constant flow, constant shear of flow and non constant shear of flow.

It is well known that the radial profile of the ITG toroidal modes is determined by the logarithmic derivative of the ion temperature and the safety factor, the modes trying to maximize the drive of the temperature gradient, while minimizing their $k_{\|}$. It is also very well known that the ITG toroidal modes do balloon in the region of unfavorable magnetic curvature, that is around $\theta \approx 0$. From now on, we will use $\{s_o, \theta_o\}$ to name the normalized radius and poloidal angle where the mode amplitude is maximum.

We can now describe the shapes of $u(s)$ that we considered. There are three basic cases: in the first one, that we will call "constant flow", the shape is simply given by: $u_0 = 1$, $u_1 = 0$, $u_2 = 0$; it has no shear at all. The second shape, that we will call "constant shear", is given by: $u_0 = -s_o$, $u_1 = 1$, $u_2 = 0$; the flow vanishes at s_o, but it has constant shear. The third shape, that we will call "non constant shear", is given by: $u_0 = \frac{1}{2}s_o^2$, $u_1 = -1$, $u_2 = \frac{1}{2}$. The flow and its constant shear both vanish at s_o, but the profile being parabolic, the second derivative of flow is not vanishing there. The three profiles are plotted in Fig.1. For each of them, the "driving terms" (the value of flow, the first derivative of flow and the second derivative respectively) have all the same value at s_o: Mach $\cdot\, v_{thi}$.

Let us first see the effect of the $E \times B$ flow on the growth rate γ of a toroidal ITG mode. Results are shown in Fig.2, where we can compare the different profiles of flow. Clearly, both the flow and its constant shear do exhibit a strong stabilizing effect, while the non constant shear seems irrelevant. We will now discuss into more details what happens for each profile.

The "constant flow" profile produces obviously the strongest stabilization. Let us explain the mechanism of this effect. As shown in Fig.5, putting the plasma into an uniform poloidal rotation does move the region θ_o where the mode balloons. A positive value of Mach number means a poloidal rotation in the direction of increasing θ, which thus increases θ_o. The consequence of which is to move the mode maximum amplitude region away from the unfavorable magnetic curvature region, reducing therefore the instability. A negative Mach number means a poloidal flow in the direction of decreasing θ, thus decreasing θ_o. At low negative values of Mach number, θ_o is first moved to a more unfavorable position, thus destabilizing the ITG. But, for stronger Mach number, θ_o moves further, leaving the unfavorable region, finally producing a strong stabilization of the toroidal ITG.

The "constant shear" profile produces also a strong stabilization, but needs stronger Mach number to be effective. Let us describe qualitatively what happens for positive values of Mach number. As can be seen in Fig.6, the value of flow itself being zero at s_o, θ_o stays approximatively constant. But there is a strong radial effect: at low Mach numbers, the mode is almost not affected by the presence of constant shear, but it cannot stand increasing Mach numbers and is finally cut in two around s_o and has to choose on which side to stay. The fact that the mode maximum amplitude region is moved away from s_o explains the stabilizing effect, as the mode is forced to see a smaller temperature gradient and as his $k_{||}$ increases, because the mode is no longer sitting on the resonant surface.

The "non constant shear" has clearly no relevant effect. It does a "little something", but this could easily be explained by the fact that around s_o, this profile has some non vanishing value of flow and of constant shear and we know they both produce strong effects.

Now we would like to briefly describe the effect of the $E \times B$ flow on $k_\perp$, that we can estimate by averaging over the eigenmode: $k_\perp^2 = \langle \nabla_\perp \delta\phi^\star \cdot \nabla_\perp \delta\phi \rangle / \langle \delta\phi^\star \delta\phi \rangle$. The results are plotted in Fig.3, where we again see that the "constant flow" has the strongest influence, nevertheless "constant shear" exhibits also a strong effect, while "non constant shear" is irrelevant. The increase of $k_\perp$ is very important: it reaches a factor two, which means that the radial extent of the mode has to be divided by two.

Again, one can look at Fig.5 to see the effect of the "constant flow". For positive Mach numbers, the smooth "fingers" become very rough, thus increasing $k_\perp$, while for negative values of Mach number, the radial extent of the mode strongly shrinks. On Fig.6, we see also that the "constant shear" significantly reduces the radial extent of the fingers, by cutting the mode in two.

As Fig.4 shows, the combination of the decrease of the growth rate γ and the important reduction of the radial extent of the fingers, has a multiplicative effect on the mixing-length estimate for the diffusion coefficient: $D = \gamma / k_\perp^2$, which is reduced by more than an order of magnitude, for both the constant flow and constant shear.

Finally, we have considered more complex shapes of the $E \times B$ profile, but nothing new happened. Profiles having both a value of flow itself and of shear at s_o were stabilizing, but less efficient than the constant flow alone, and usually more efficient than the constant shear by itself.

IV. CONCLUSION

The first global and kinetic study of $E \times B$ flows on the linear stability of ITG modes has been presented. It shows that:

- $E \times B$ flows have a very strong stabilizing effect on toroidal ITG modes,
- they also strongly reduce the radial extent of the convective cells,
- only the intensity of the flow and its first derivative have an effect,
- for instance, the second derivative of flow (or curvature of flow) does not have any relevant effect.

We have seen that the flow can have both a radial and a poloidal influence on the ITG modes, both effects being important and qualitatively quite different, which fully justifies the global resolution of the gyrokinetic equation.

Remaining questions to be answered include the study of what happens when the magnetic shear becomes negative and the effect of $E \times B$ flows on trapped particles modes.

Acknowledgment: this work was in part supported by the Swiss National Science Foundation.

REFERENCES

[1] K.H. Burrell, Physics of Plasmas **4**, 1499, (1997)

[2] J.B. Taylor, H.R. Wilson, Plasma Phys. Control. Fusion **38**, 1999, (1996)

[3] M.Maccio, J. Vaclavik and L. Villard, in *Theory of Fusion Plasmas, Int. Workshop, Varenna, September 1998* (Editrice Compositori, Società Italiana di Fisica, Bologna, 1999), p.511

[4] T.S. Hahm, Physics of Plasmas **3**(12), 4658, (1996)

[5] S.Brunner, M. Fivaz, T.M. Tran and J. Vaclavik, Physics of Plasmas **5**(11), 3929, (1998)

[6] S.Brunner, J. Vaclavik, Physics of Plasmas **5**(2), 365, (1998)

FIGURE CAPTIONS

Fig.1 The three different shapes of $E \times B$ flow.

Fig.2 Growth rate as a function of Mach number, $\omega_{norm} = v_{thi}^2/[\omega_{ci}a^2]$.

Fig.3 $k_\perp$ as a function of Mach number, at ρ_L constant.

Fig.4 Mixing-length estimate for the diffusion coefficient as a function of Mach number.

Fig.5 Evolution of the ITG mode in the poloidal plane, "constant flow" profile.

Fig.6 Evolution of the ITG mode in the poloidal plane, "constant shear" profile.

FIGURES

FIG.1 Maccio

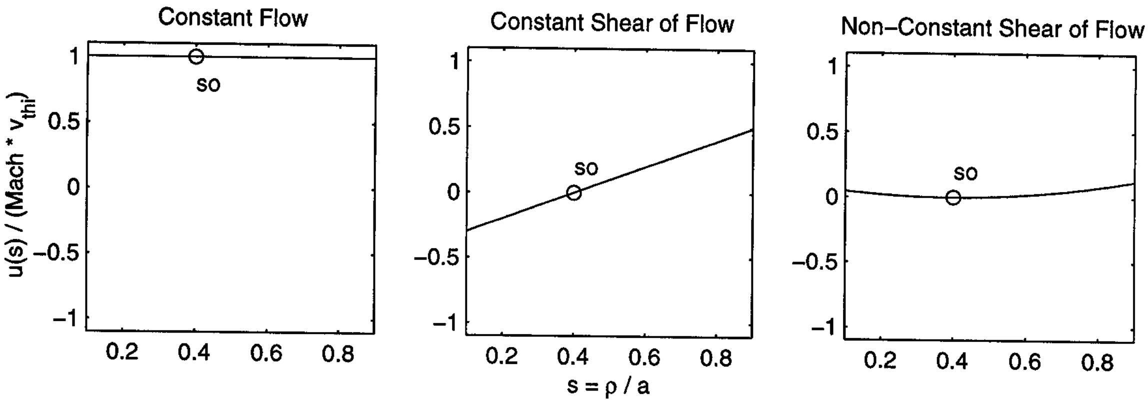

FIG.2 Maccio

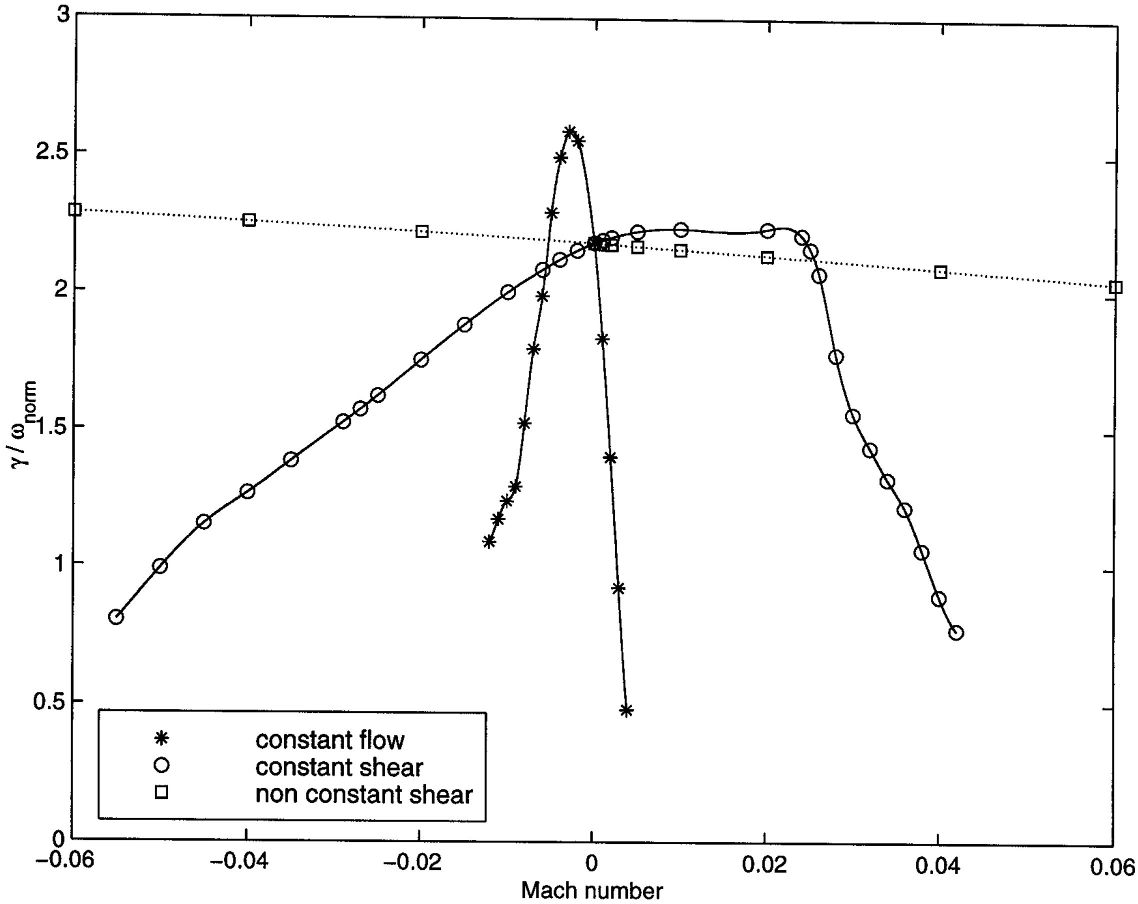

3
2.5
2
1.5
1
0.5
0
−0.06
−0.04
−0.02
0
0.02
0.04
0.06
Mach number
γ / ω_norm
constant flow
constant shear
non constant shear

FIG.3 Maccio

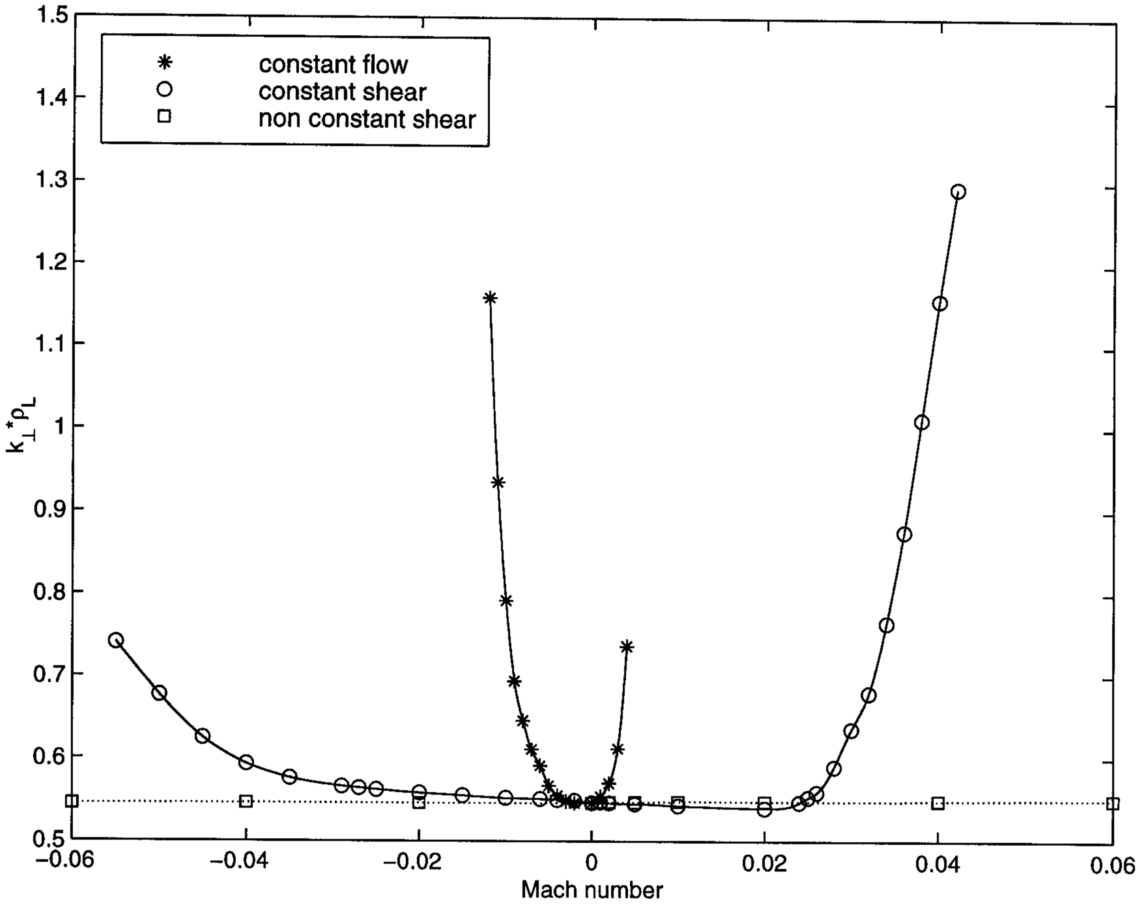
constant flow
constant shear
non constant shear
$k_\perp{}^*\rho_L$
Mach number
1.5
1.4
1.3
1.2
1.1
1
0.9
0.8
0.7
0.6
0.5
−0.06
−0.04
−0.02
0
0.02
0.04
0.06

FIG.4 Maccio

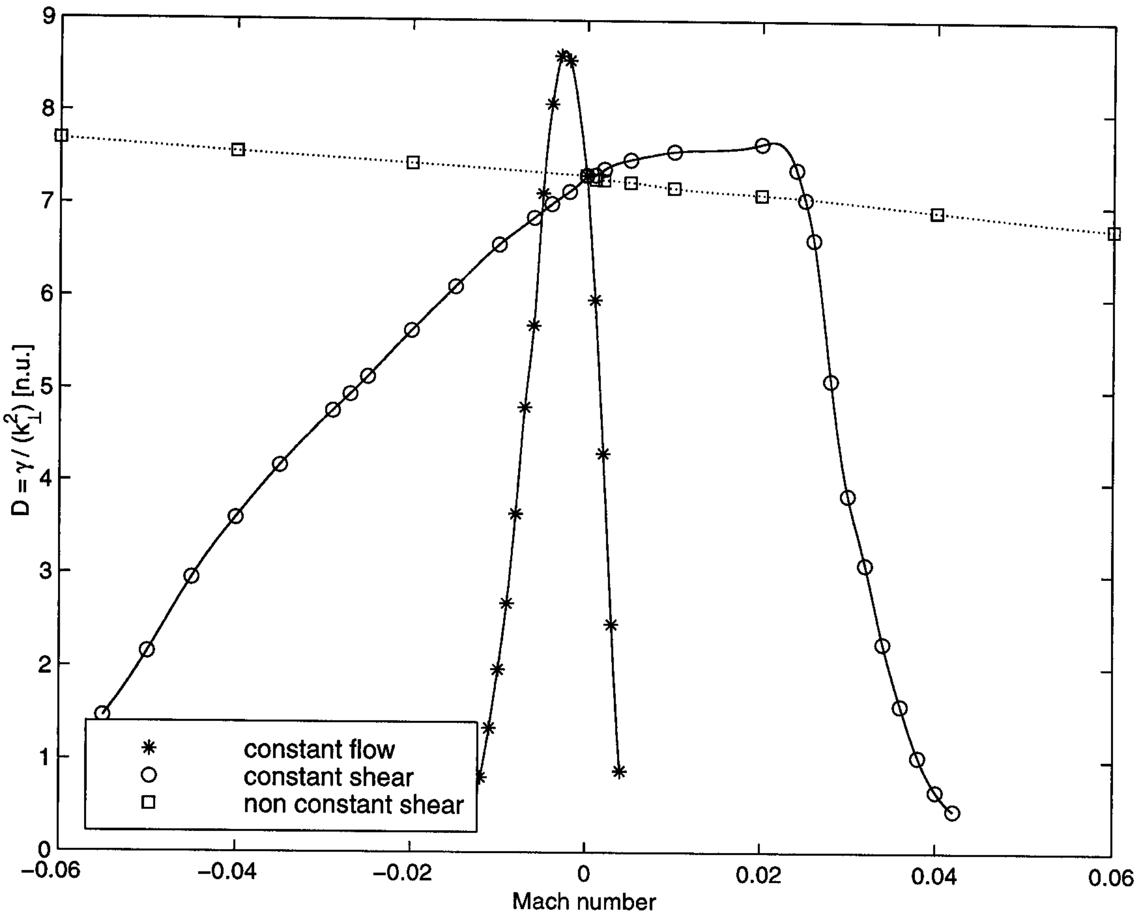

9
8
7
6
5
4
3
2
1
0
D = γ / (k⊥²) [n.u.]
−0.06
−0.04
−0.02
0
0.02
0.04
0.06
Mach number
constant flow
constant shear
non constant shear

FIG.5 Maccio

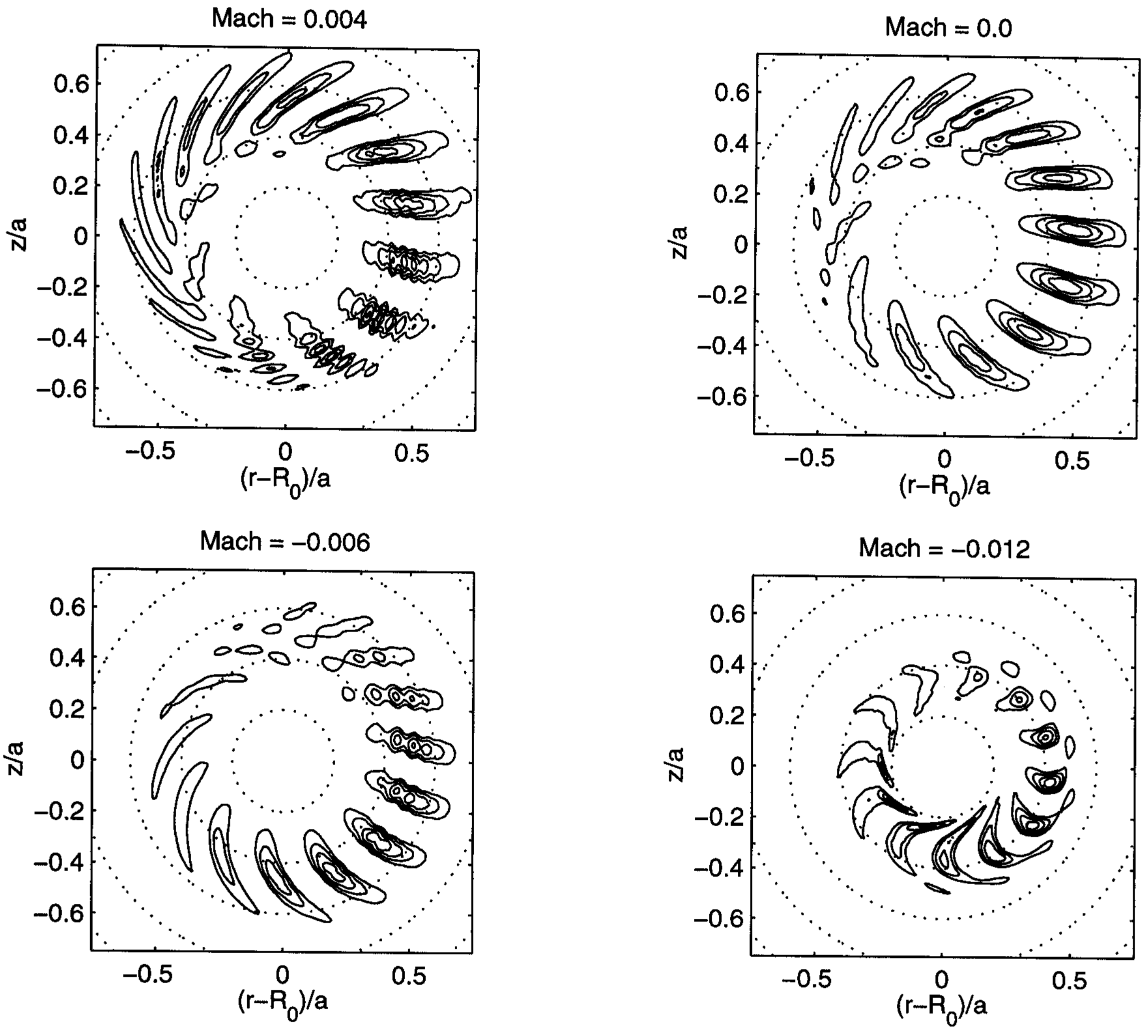
Mach = 0.004
Mach = 0.0
Mach = −0.006
Mach = −0.012
z/a
(r−R0)/a
0.6
0.4
0.2
0
−0.2
−0.4
−0.6
−0.5
0.5

FIG.6 Maccio

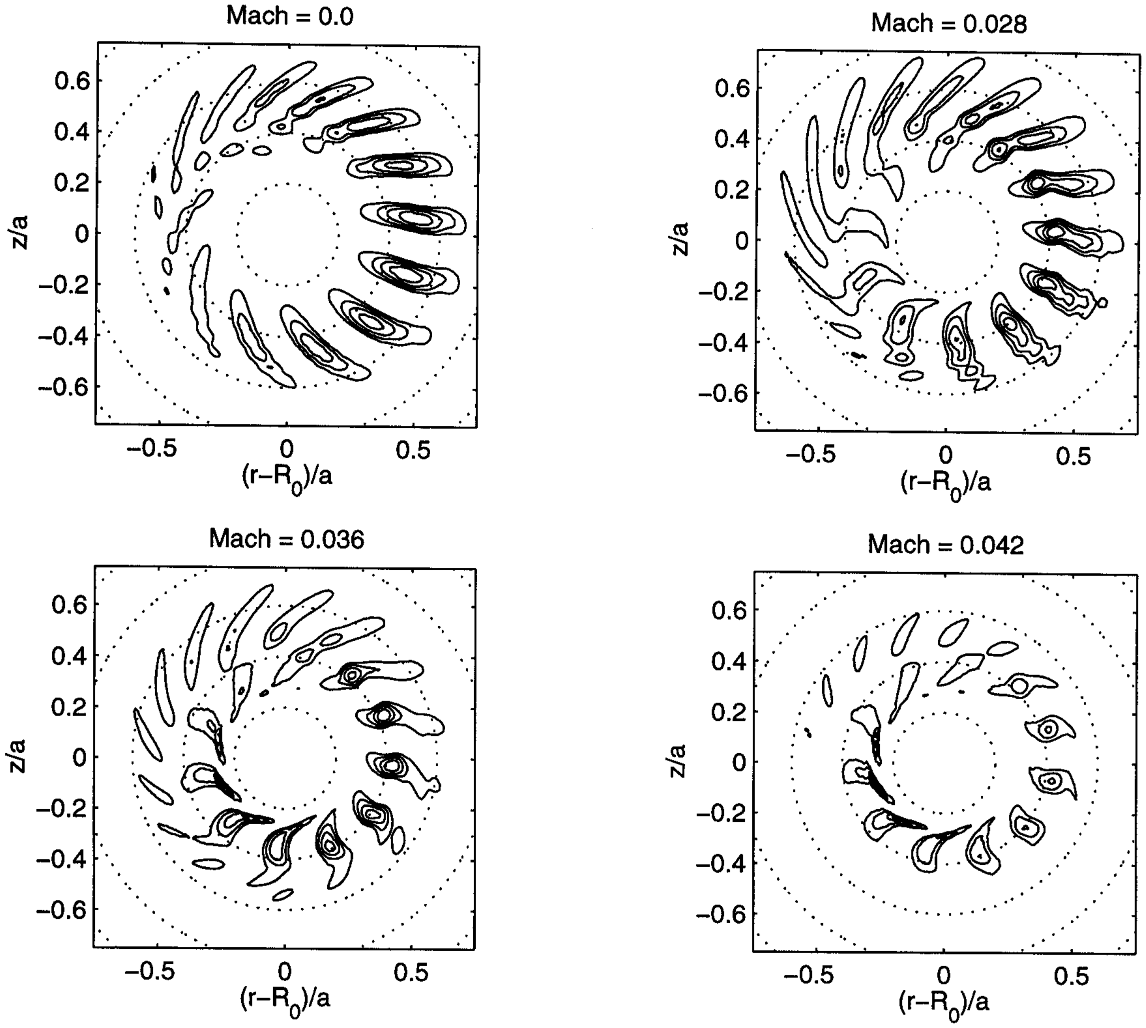
Mach = 0.0
Mach = 0.028
Mach = 0.036
Mach = 0.042
z/a
(r−R$_0$)/a
0.6
0.4
0.2
0
−0.2
−0.4
−0.6
−0.5
0.5